

Numerical Investigation of Ohmic Heating in Channel Flow

E. A. Salih¹, S. Y. Spotar²

¹Department of Food Engineering, Faculty of Engineering, University of Geziera, Sudan.

²Department of Chemical Engineering, Faculty of Engineering, University Nottingham, Malaysia

Corresponding author. Email: elzubiersalih@yahoo.com

ABSTRACT

Heat generation by direct electric conduction (ohmic heating) in a fully developed channel flow was studied to evaluate interaction between the hydrodynamic, electric and the thermal phenomena involved under the effect of natural convection. The equations governing the system were solved numerically by CFD finite volume code (FLUENT6.1 software package). The velocity profiles accelerate more near the wall than at the center that makes the temperature distribution uniform in the channel span. The numerical model is validated with an earlier experimental study [El Moctar *et al.* 1996] and yielded good agreement.

Key word: Ohmic heating, Mixed convection, Heat generation, Numerical modeling.

INTRODUCTION

Ohmic heating technology has been investigated for heating of various materials for a long time. The basic principle of ohmic heating is that electrical energy is converted to thermal energy within a conductor. Typically, an alternating current is applied across the material. Because heating occurs by internal energy generation within the conductor, the method results in a more even distribution of temperatures within the material compared with conventional heating through the wall.

Attempts to apply ohmic heating have mainly been focused in the food industry, where the speed and uniformity of heating is an advantage for technology operations such as sterilization, defrosting, bleaching, cooking, etc (De Alwis, *et al.*, 1989).

The process of volume heating by direct electric conduction is generally classified

as being in the field of electro hydrodynamics coupled with heat transfer (Jones, 1978) or 'thermo-electro-hydrodynamics' (TEHD), a subject that has been the focus of intensive research since the 1930s (Senftleben and Braun, 1936). Those investigations were mostly oriented towards applications in traditional heat exchangers with the specific purpose of developing new liquids which could be used in heat exchangers. They were concerned with the increase of the heat transfer coefficient on a heated surface caused by the application of an electric field, and also often involved an electrically insulating liquid. However, these studies provided an opportunity to characterize the coupling between electric and thermal fields in various situations. The same configurations were also used to study the coupling between the electric and hydrodynamic fields via the highly interesting phenomenon of electro conductive instability (Turnbull, 1971).

The objective of this study is to model ohmic heating in channel flow using commercial CFD software package (FLUENT 6.1) and compare it with accurate (more than 95%) and well documented experimental data obtained by using of laser Doppler anemometry and flow visualization by laser-induced fluorescence (LIF) technique (El Moctar, 1996).

MODELING AND SIMULATION

The flow under consideration is shown in Fig.1; it is the flow that has been experimentally studied [5]

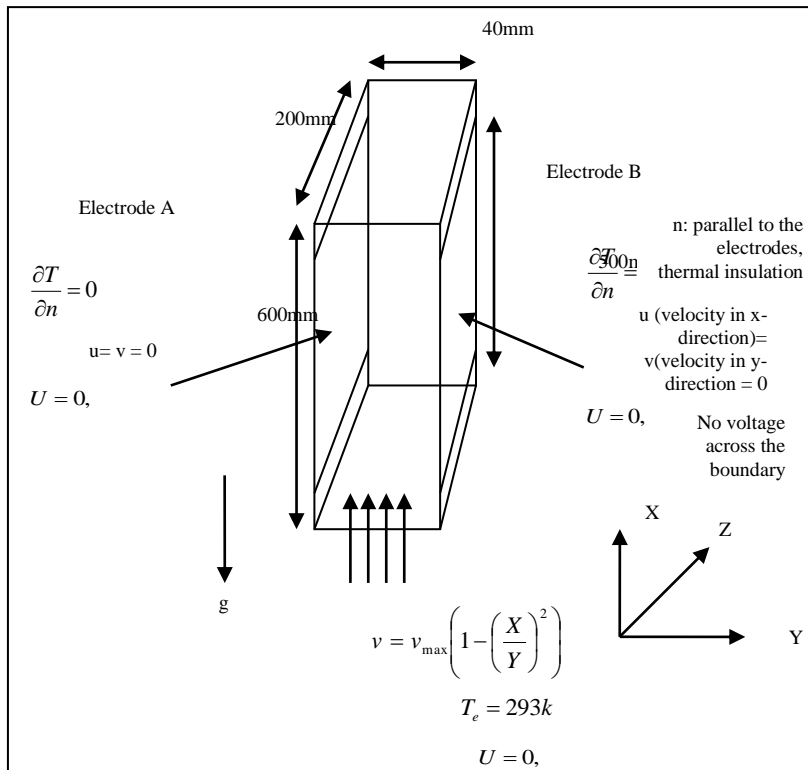


Figure 1. The geometry and the boundary conditions for the flow under considerations

and it is assumed that the flow is modeled by the solution of the following equations
Continuity equation (overall mass balance)

$$\frac{\partial}{\partial x} (\rho u) + \frac{\partial}{\partial y} (\rho v) = 0 \quad (1)$$

Momentum balance in x direction (parallel to plate (electrode) and gravity) for a

Newtonian fluid with constant ρ and μ .

$$\rho \left[u \frac{\partial u}{\partial x} + v \frac{\partial u}{\partial y} \right] = - \frac{\partial p}{\partial x} + \mu \left[\frac{\partial^2 u}{\partial x^2} + \frac{\partial^2 u}{\partial y^2} \right] - \rho g_x \quad (2)$$

We have already used approximation (1) in choosing which version of the equations to copy from the text. In approximation (2), we say that there is no pressure gradients

perpendicular to the plate. This means that the axial pressure gradient, $\frac{\partial P}{\partial x}$ is independent

of y , far from the plate, where the velocity is zero, this pressure gradient is just the hydrostatic pressure gradient:

$$\frac{\partial P}{\partial x} = -\rho_{\infty} g_x \quad (3)$$

Substituting this hydrostatic pressure gradient into the momentum balance gives

$$\rho \left[u \frac{\partial u}{\partial x} + v \frac{\partial u}{\partial y} \right] = \mu \left[\frac{\partial^2 u}{\partial x^2} + \frac{\partial^2 u}{\partial y^2} \right] + (\rho - \rho_{\infty}) g_x \quad (4)$$

Now, we apply assumption (3), the Boussinesq approximation. This says that we can write the density variation as

$$(\rho - \rho_0) = \rho_0 \beta (T - T_0) \quad (5)$$

$$\rho = \rho_0 [1 + \beta (T - T_0)] \quad (6)$$

where $\beta(T - T_0) \ll 1$

Where β is the coefficient of thermal expansion of the fluid, defined as

$$\beta = -\frac{1}{\rho} \left(\frac{\partial \rho}{\partial T} \right) \Big|_{T=T_{\infty}} \quad (7)$$

Applying the Boussinesq approximation to the momentum equation gives

$$\rho \left[u \frac{\partial}{\partial x} + v \frac{\partial}{\partial y} \right] = -\frac{\partial p}{\partial x} + \mu \left[\frac{\partial^2 u}{\partial x^2} + \frac{\partial^2 u}{\partial y^2} \right] + \rho g_x \beta (T - T_{\infty}) \quad (8)$$

Energy balance for a Newtonian fluid with constant ρ and μ .

$$\rho C_p \left[u \frac{\partial T}{\partial x} + v \frac{\partial T}{\partial y} \right] = k \left[\frac{\partial^2 T}{\partial x^2} + \frac{\partial^2 T}{\partial y^2} \right] + Q \quad (9)$$

and the Laplace equation of electric field [5] is

$$\frac{\partial}{\partial x} \left(\sigma_x(T) \frac{\partial U}{\partial x} \right) + \frac{\partial}{\partial y} \left(\sigma_y(T) \frac{\partial U}{\partial y} \right) = 0 \quad (10)$$

Finally, according to equation (4), we can neglect the diffusive terms in the x -direction.

Doing this, dividing the continuity and momentum equations through by the density, and

dividing the energy equation through by the density and specific heat gives us the governing equations that we will use to analyze this situation.

An electrical characteristic number El could be used to replace the Grashof number to model the electrically induced natural convection:

$$Gr = \frac{g\rho^2\beta L^3\Delta T}{\mu^2} \quad (11)$$

$$El = \frac{\rho^2\beta bL^2\Delta TE^2}{\mu^2}$$

(12)

(13)

$$g = \frac{bE^2}{L}$$

The temperature gradient across the flow can also give rise to natural convection which is superposed on the base flow and results in a mixed convection regime. The Richardson number $Ri = Gr/Re^2$, defined as the ratio between the Grashof number and the square of the Reynolds number, measures the relative importance of free convection with respect to the forced convection.

The boundary conditions corresponding to the case under consideration here are summarized in Fig.1 and are Hydrodynamic, thermal and electrical boundary conditions.

1. Boundary conditions:

1.1. Hydrodynamic boundary conditions: This consists of: a non-slip, non-penetration condition on the wall: $u = v = 0$; an imposed velocity profile at the input and the boundary condition at the output is given by the solution to the convection and verification of the conservation of mass.

1.2. Thermal boundary conditions:

These consist of: uniform temperature T_{in} at the input to the flow field and thermal insulation condition $\frac{\partial T}{\partial n} = 0$ at the output and on all walls including the electrodes.

The latter condition is not realistic, but we consider that the electrodes are thin and backed by an insulating material, we can then ignore the heat transferred by conduction perpendicular to the electrodes and in the horizontal and vertical directions.

1.3. Electrical boundary conditions:

These consist of: zero electrical potential on electrode B maintained a potential U_0 . Electrical insulation condition is assumed on all other walls.

The physical properties of the working fluid (table (1)) used in the simulation were taken as in the experimental work [5]

Table [1] the physical properties of the working fluid

ρ	996.84 kg/m ³
C_p	4185 J/kgK
μ	0.0008843 kg/ms
k	0.61 W/mK
σ	0.0275 S/m

The mean velocity ($V_m = 0.0073$ m/s), the voltage applied ($U = 242.5$ volts) and the temperature range ($T_{in} - T_{out} = 10.46$ K) they were taken from [5].

2. Assumptions:

To solve the governing equations the following assumptions are used

- (1) Constant properties (μ , k , C_p), except for the variation in density (see equation 4) that drives the flow. This means the flow is incompressible with density fluctuation
- (2) Pressure gradients perpendicular to the plate (electrode) can be neglected.
- (3) Density variation can be approximated by a linear dependence on temperature. This is called the Boussinesq approximation (see below).

(4) Diffusive transport (of both momentum and energy) in the direction parallel to the plate (electrodes) can be neglected. There are also, of course, many other implied assumptions (steady-state situation, viscous dissipation is negligible in the energy equation; everything is constant in the z -direction

(5) The flow is fully developed channel flow with two electrode walls, and two dimensional.

(6) Fluid enters the channel at constant temperature T_{in} .

RESULTS

Commercial software FLUENT is used to solve the governing equations. The test section is a rectangular duct of $40\text{mm} \times 200\text{mm}$ cross-sectional and 600mm length. The two $40\text{mm} \times 600\text{mm}$ walls are transparent, while the other two $200\text{mm} \times 500\text{mm}$ walls are made of the metal constituting the electrodes Fig.1. User defined function is used to customize FLUENT for parabolic inlet velocity.

The mesh size of the geometry is 4400 cells which is 4641 nodes

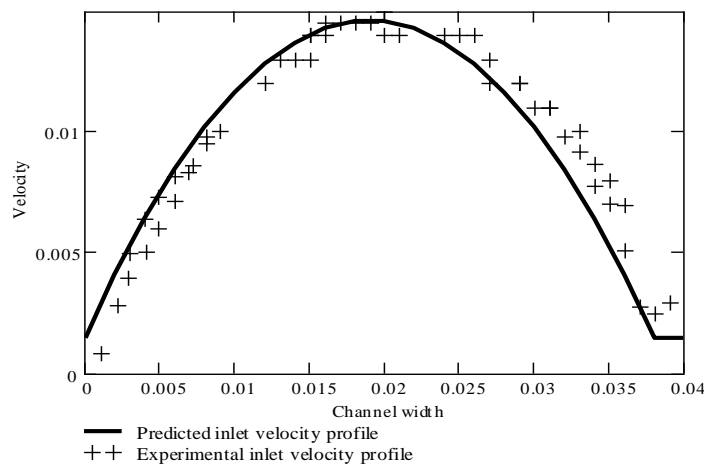


Figure 2. Comparison of predicted by FLUENT and experimental inlet velocity

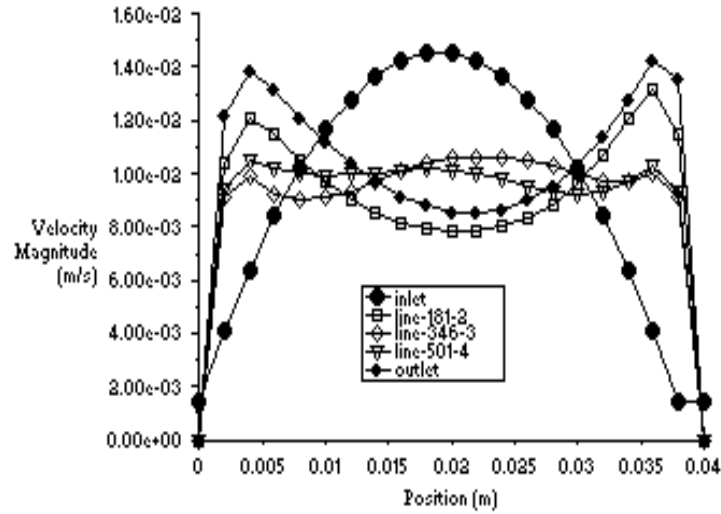


Figure 3. Predicted velocity profiles with natural convection at different locations of the system

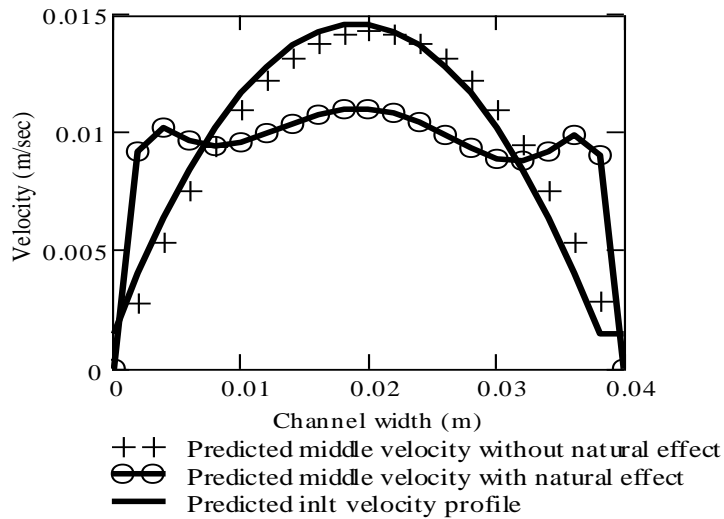


Figure 4. Comparison of middle velocity with and without natural convection

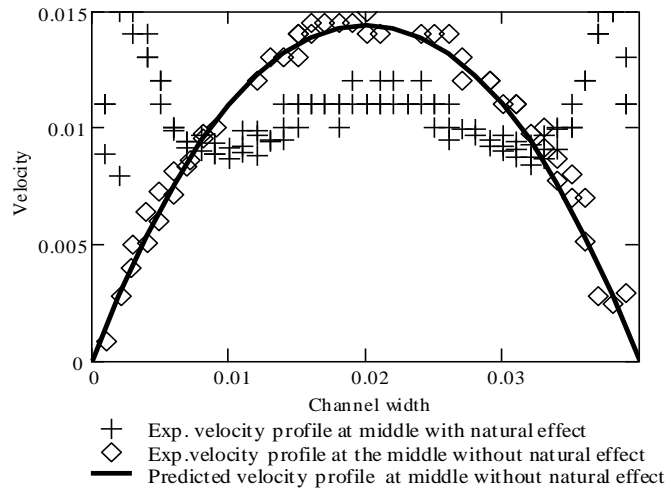


Figure 5. Comparison of predicted and experimental middle velocity with without natural convection

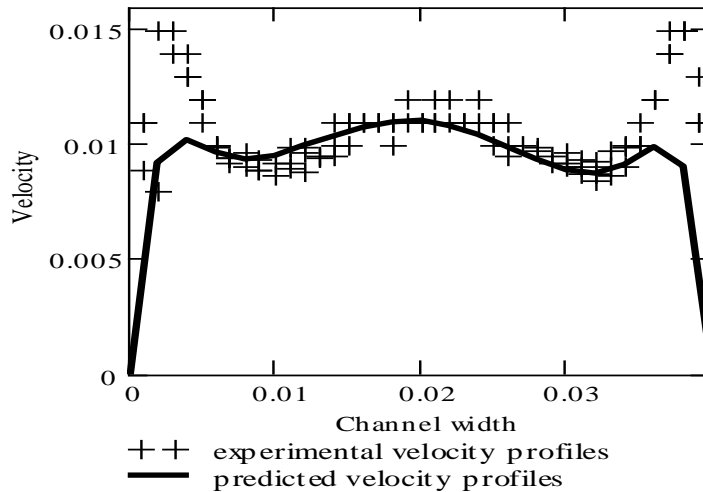


Figure 6. Comparison between predicted and experimental velocity profiles at the middle of the system

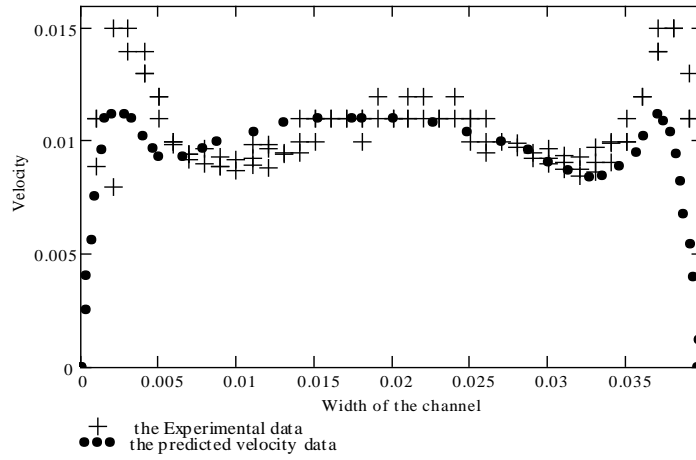


Figure 7. Comparison between predicted and experimental velocity profiles at the middle of the system

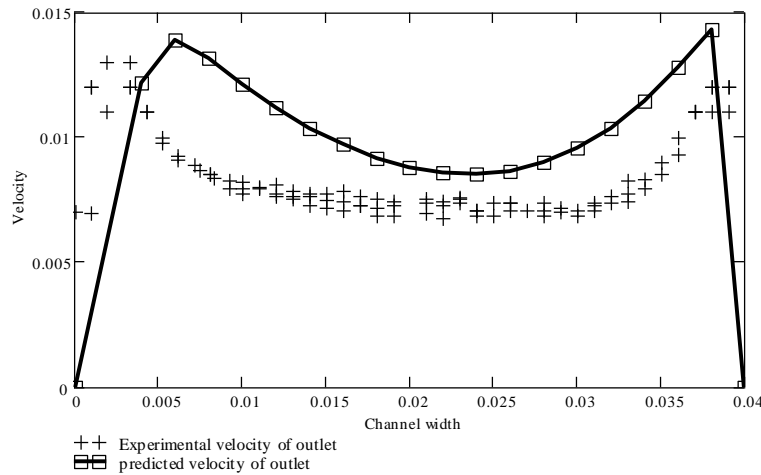


Figure 8. Comparison between experimental and predicted outlet velocity profiles

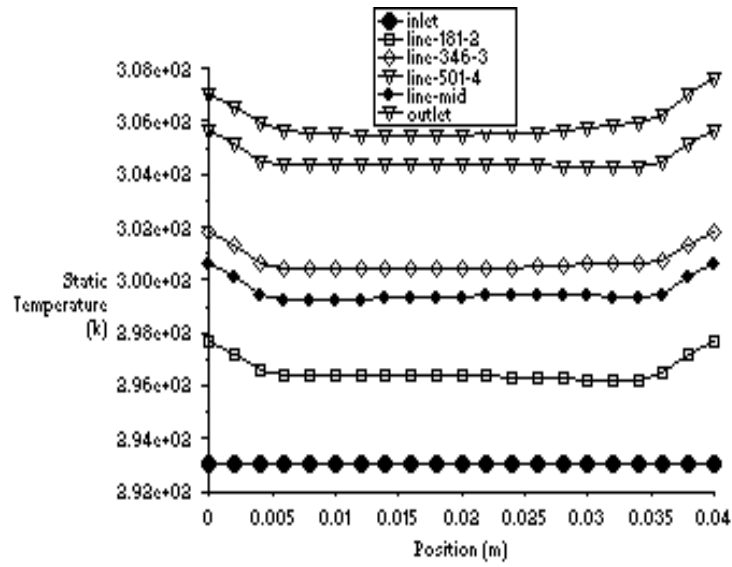


Figure 9. Temperature profiles at different distance from the entrance to test section with free convection

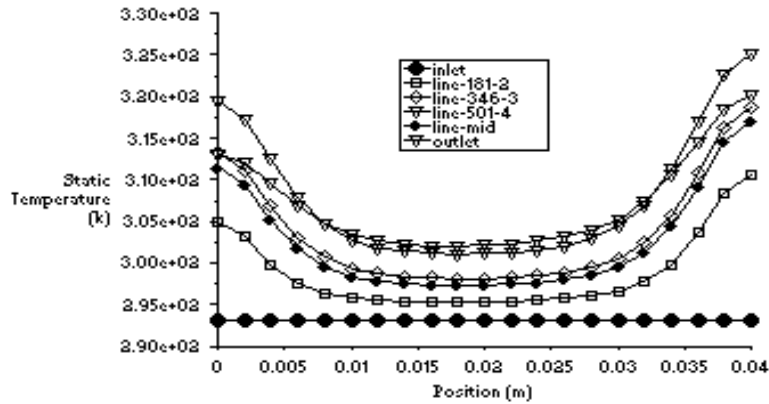


Figure 10. Temperature profiles at different distance from entrance to test section without free convection

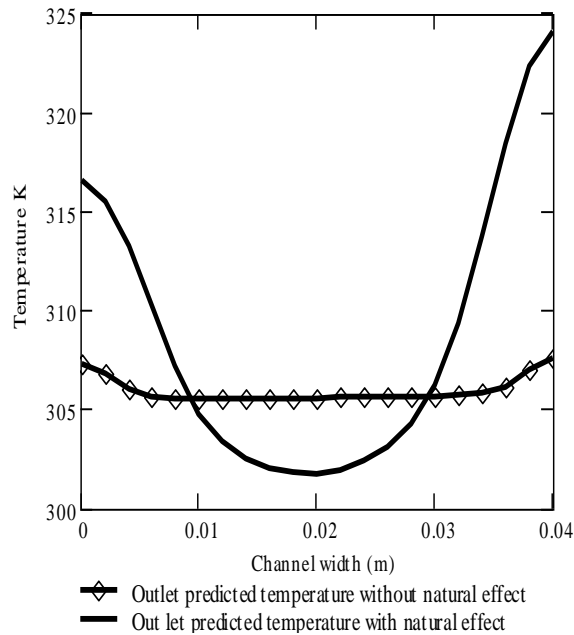


Figure 11. Temperature profiles of exit with and without free convection

DISCUSSION

Fig.2 shows the comparison between the predicted and experimental inlet velocity profile computed by Fluent and by [5]. Fig.3 shows the comparison of the velocity profiles at different locations of the system.

Velocity profiles at entrance to and middle of test section. Fig.4 shows comparison of middle velocity with and without natural convection. Fig 5 shows comparison between experimental middle velocity with and without natural convection and predicted one. Fig.6 shows comparison between predicted and experimental velocity profiles at the middle of the system. Fig.7 shows the comparison between predicted and experimental of the velocity profiles at the middle of the system done by [5]. Fig. 8 shows the comparison of experimental and predicted outlet velocity profile. Fig.9 shows the temperature profiles at different distance from the entrance to test section with free convection effect. Fig.10 shows the temperature profiles at different distance from entrance to test section without free convection effect and Fig. 11 shows the temperature profiles of exit with and without free convection effect.

So the flow velocity is much higher at the middle of the channel than in the vicinity of the walls. The fluid passing in the vicinity of the walls remains longer under the influence of the electric field and are heated more than those traveling faster in the middle of the channel. This difference in the residence time cause a temperature gradient between the center of the flow and the vicinity of the walls. The horizontal temperature gradient is added to the progressive heating of the liquid that takes place as it passes through the channel. The special form of the velocity profile in the channel mid-height can be explained by the effect of the horizontal temperature gradient. Due to the buoyancy effect the fluid particles in the vicinity of the wall travel faster, in comparison to those in the input velocity profile, due to smaller density, and hence natural convection arises. Fluid particles in the channel center, on the contrary, move more slowly since they have not been under the effect of electric field as long as the particles close to the walls. This trend is reversed farther downstream, as discussed below.

The effect of the natural convection is an acceleration of the hot liquid in the vicinity of the wall; in other words, there is a noticeable decrease in the thickness of the boundary layer. A direct consequence of this acceleration is that the velocity becomes more uniform in any given section of the channel compared with the parabolic profile imposed at the input travel faster.

Fig.9 shows the temperature profiles at different distance from the entrance to test section with free convection and it is uniform because of the buoyancy effect. Fig.10 shows the temperature profiles at different distance from entrance to test section without free convection and in this case the temperature is not uniform. Fig 11 shows the comparison of temperature at exit with and without the buoyancy effect, and the temperature under the buoyancy effect is more uniform than that without the effect of the buoyancy effect.

CONCLUSION

The commercial software FLUENT 6.1 with MHD module when is used for modeling the ohmic heating of fluid flow in a channel gave close results (velocity profiles curves) to that calculated by other methods [5]

NOMENCLATURE

- X Any distance along the half width of the channel
- Y The half of the channel width
- C_p Specific heat (J/kgK)
- k Thermal conductivity (W/mK)
- m Temperature coefficient
- Q Internal energy source (W/m³)
- T Temperature (K)
- T_0 Reference means temperature (K)
- t Time (s)
- U_0 Applied electric potential (v)
- U Voltage (v)
- σ Electrical conductivity (S/cm)
- σ_0 Referencing electrical conductivity (S/cm)
- ρ Density (kg/m³)
- E Electrical field (v/m)
- E_1 Electrical Grashof numbers
- f Frequency (Hz)
- f_e Electric force (N)
- \vec{g} Gravitational acceleration (m/s²)
- Gr Grashof number
- H Electrode length (m)
- I Current intensity (A)
- L Inter electrode distance (m)
- P Pressure (Pa)
- Ra Raleigh number
- Re Reynolds number
- Ri Richardson number
- T_{in} Temperature at the entrance to the channel (K)
- T_{out} Temperature at the channel exit section (K)
- u Span wise velocity components (m/s)

- v Stream wise velocity components (m/s)
 \vec{V} Velocity vector (m/s)
 V_m Mean stream wise velocity (m/s)

REFERENCES

- De Alwis, A. A.; P. K. Halden, and P. J. Fryer** (1989). Shape and conductivity effects in the Ohmic heating of foods, *Chem. Engng Res. Des.* 67,1599-192.
- El Moctar, A. Ould; H. Peerhossaini and J. P. Bardou** (1996). Numerical and experimental investigation of direct electric conduction in a channel flow *Int. J. Heat and Mass Transfer* 1. 39, No. 5, pp. 975-993.
- Jones, T. B.** (1978). Electrohydrodynamically enhanced heat transfer in liquids-A review, *Adv. Heat Transfer* 14:107-148.
- Senftleben, H. and W. Braun** (1936). Der Einfluss elektrischer Felder auf den Wärmestrom in Gasen, *Z. Phys.* 102, 480-500.
- Turnbull, R. J.** (1971). Effect of a non-uniform alternating electric field on the thermal boundary layer near a heated vertical plate, *J. Fluid Mech.* 49,693-703.

ملخص الدراسة

توليد الحرارة بالتوصيل الكهربائي المباشر (التسخين الاومي) في قناة ذات التدفق المتطور الكامل ، درس لتقييم التفاعل بين الظواهر الكهربائية و الحرارية الهيدروديناميكية تمت تحت تأثير إنتقال الحمل الطبيعي للحرارة ، المعادلات التي تحكم النظام حلت باستخدام برنامج CFD (FLUENT 6.1). تسارعت السرعة أكثر قرب الحائط من المركز التي تجعل توزيع درجة الحرارة بانتظام في مدى القناة. إنَّ النموذج العددي مصدق بدراسة سابقة [ولد المختار و اخرون] أنتج إتفاقية جيدة.